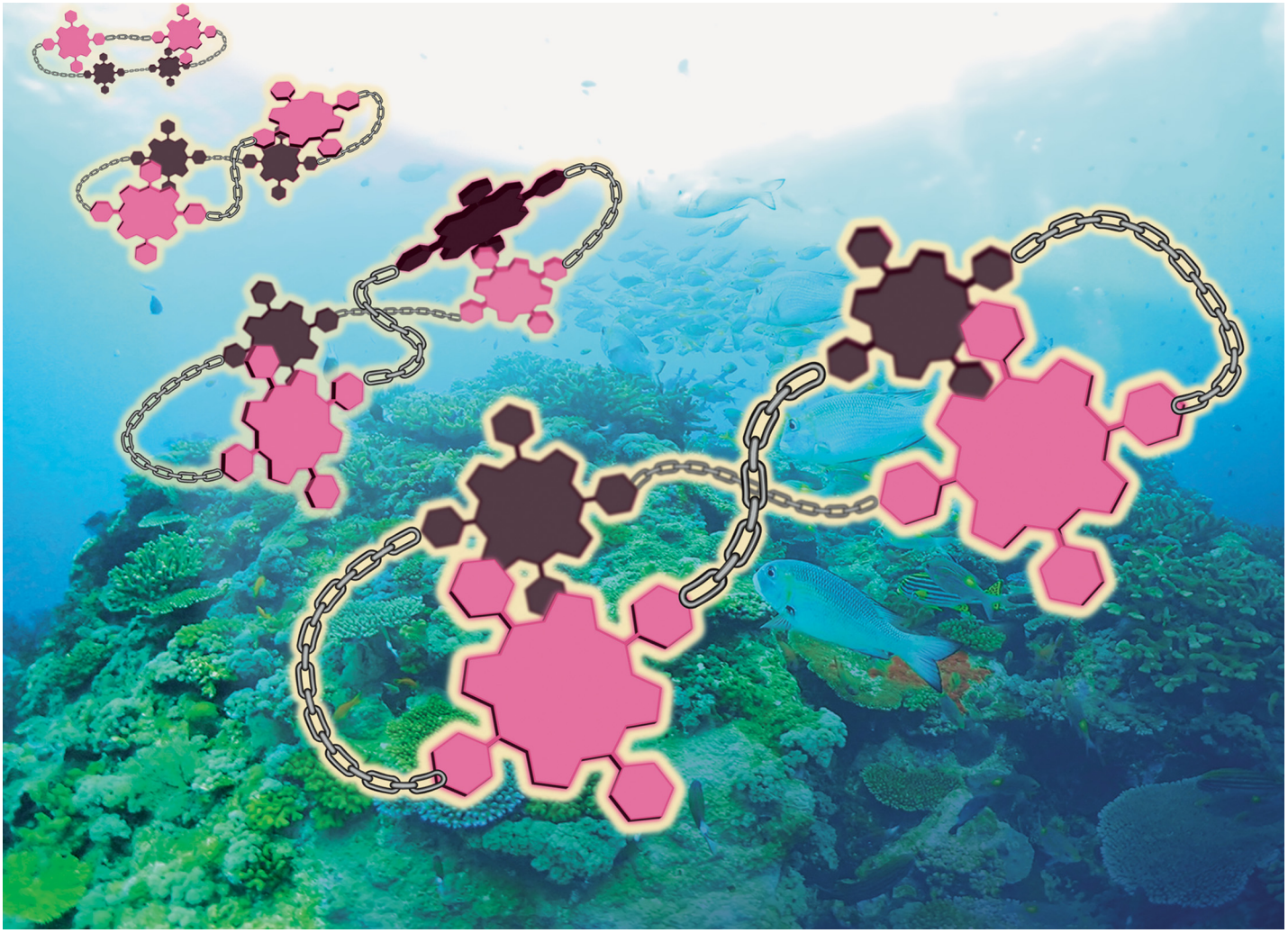

Showcasing research from the laboratories of Professor Fukuhara, Institute for Materials Chemistry and Engineering, Kyushu University, Japan.

A chiroptical switcher: helical inversion of twisted porphyrin macrocycle synergistically controlled by combined stimuli of solvent and pressure

In this study, we revealed that a chirally twisted porphyrin macrocycle shows dynamic chiroptical switching in response to hydrostatic pressure. The anisotropy factor (*g*) is tuned or even inverted depending on solvent polarity, highlighting how molecular flexibility and solvation synergistically govern pressure responsiveness.

Image reproduced by permission of Gaku Fukuhara from *Chem. Commun.*, 2025, **61**, 18340.

As featured in:

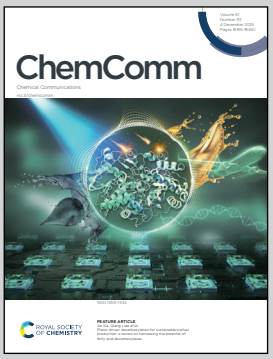

See Takeharu Haino, Gaku Fukuhara *et al.*, *Chem. Commun.*, 2025, **61**, 18340.

ROYAL SOCIETY OF CHEMISTRY

rsc.li/chemcomm

Registered charity number: 207890

ChemComm

COMMUNICATION

View Article Online
View Journal | View Issue

Cite this: *Chem. Commun.*, 2025, **61**, 18340

Received 22nd September 2025,
Accepted 21st October 2025

DOI: 10.1039/d5cc05443e

rsc.li/chemcomm

A chiroptical switcher: helical inversion of twisted porphyrin macrocycle synergistically controlled by combined stimuli of solvent and pressure

Tomoyuki Hamachi,†[a] Tomokazu Kinoshita,†[b] Kouta Tanabe,[cd] Naoyuki Hisano,[c] Takeharu Haino *[cd] and Gaku Fukuhara *[ab]

Herein, we report the unprecedented discovery of 1 that possesses dynamically tunable chiroptical properties under hydrostatic pressure. Upon hydrostatic pressurization, the *g* factor inverts from negative to positive. These chiroptical switches are based on pressure-induced conformational change governed by the interplay between macrocyclic flexibility and solvent polarity.

Chiral organic dyes and synthetic π-conjugates often exhibit interesting optically active properties that can be modulated by external stimuli. The continued creation of these compounds to develop smarter materials for applications in chirality sensing, display technologies, secure optical communication, and information storage is imperative.[1–12] Their chiroptical properties can be read out with high sensitivity by optical techniques such as circular dichroism (CD) and circularly polarized luminescence (CPL). To date, a variety of chiroptical switching materials that are susceptible to solvent,[13,14] pH,[15,16] ions,[17,18] redox,[19,20] temperature,[21,22] light,[23,24] and magnetic fields[25,26] have been reported.

Among the several stimuli examined thus far, hydrostatic pressure, a type of isotropic mechanical force, can modulate the molecular conformation, solvation state, and recognition processes based on volume changes (ΔV). In recent years, the hydrostatic pressure has been rapidly gaining attention in the fields of mechanochemical sensing[27–29] and mechanobiology,[30–33] where it remains challenging to determine when, where, and how a mechanical stimulus acts. Importantly, molecules whose chiroptical responses and chiral recognition can be controlled by hydrostatic pressure are quite promising as precise chiroptical reporters for mechanical input/output, as even slight pressure-induced conformational changes can be sensitively reflected in chiroptical signals.[34–37]

Nevertheless, limited examples of pressure-controlled chiroptical switching and chiral recognition systems have been reported, which leads to the conclusion that general guidelines for the molecular design of these systems have yet to be fully established. This is because not only intrinsic structural changes but also interactions with solvent molecules strongly affect the pressure responsiveness. In particular, it is extremely difficult to predict the latter term and reflect it in molecular design. Thus, a major challenge in this field is the rational design of flexible molecular systems of which the structure and function can be dynamically controlled by the synergistic effects of solvation and hydrostatic pressure.

The tetrakisporphyrin macrocycle we focus on in this work is linked by a chiral dioxolane spacer, and combines structural flexibility with diverse solvent responsiveness.[38] The (*R*,*R*)-enantiomeric macrocycle **1** (Fig. 1) can adopt either right-handed (*P*) or left-handed (*M*) twisted conformations, the helical sense of which is known to be perturbed depending on the polarity and the structure of the solvents used. Hence, **1** is expected to exhibit pronounced conformational adaptability in response to both pressure and solvation, thus constituting an ideal platform for investigating the way in which the interplay between hydrostatic pressure and the solvent microenvironment modulates the three-dimensional structure.

We demonstrated that, under hydrostatic pressure, the chiroptical properties of **1** vary substantially, with the unprecedented outcome that the solvent-dependent chiroptical properties are inverted under hydrostatic pressurization. These results indicate that successful pressure-driven chirality control of helical structures requires not only a flexible molecular scaffold but also appropriate and rational molecular design for solvent

[a] *Institute for Materials Chemistry and Engineering, Kyushu University, 744 Motooka, Nishi-ku, Fukuoka 819-0395, Japan. E-mail: gaku@ms.ifoc.kyushu-u.ac.jp*
[b] *Department of Chemistry, Institute of Science Tokyo, 2-12-1 Ookayama, Meguro-ku, Tokyo 152-8551, Japan*
[c] *Graduate School of Advanced Science and Engineering, Hiroshima University, 1-3-1 Kagamiyama, Higashi-Hiroshima, Hiroshima 739-8526, Japan. E-mail: haino@hiroshima-u.ac.jp*
[d] *International Institute for Sustainability with Knotted Chiral Meta Matter (WPI-SKCM2), Hiroshima University, 1-3-1 Kagamiyama, Higashi-Hiroshima, Hiroshima 739-8526, Japan*
† These authors contribute equally to this work.

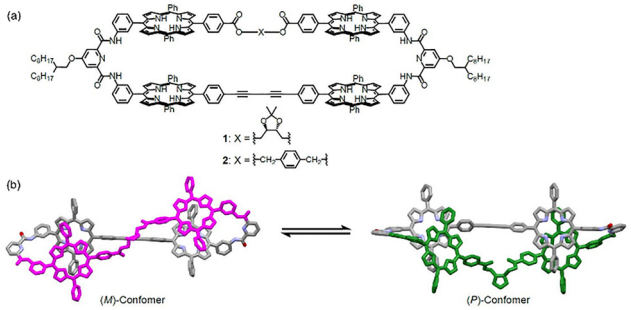

Fig. 1 (a) Molecular structures of macrocycles **1** and **2**. (b) Schematic illustration of the chiral inversion of the flexible macrocycle induced by hydrostatic pressure.

interactions. Herein, we report the serendipitous discovery that the unexpected helical inversion of the chirally twisted macrocycle is synergistically induced by the combined effect of the hydrostatic pressure and microenvironmental polarities.

First, to investigate the fundamental optical properties of the tetrakisporphyrin macrocycles, we performed hydrostatic pressure-spectroscopic measurements using the referenced achiral macrocycle, **2** (Fig. 1), which exhibited a Soret band around 420 nm and Q-bands in the ranges of 500–700 nm in both toluene and THF at ambient pressure (0.1 MPa),[39] (Fig. S2, SI). With increasing hydrostatic pressure, the Soret and Q-bands underwent steady bathochromic shifts of −0.82 and −0.39 cm^{-1} MPa^{-1} in toluene and −0.71 and −0.31 cm^{-1} MPa^{-1} in THF (Fig. S3, SI). This behavior, attributed to changes in the solvent polarizability/density under pressure,[40,41] stabilizes the polarized excited state. In addition, the hyperchromic effect is simply the result of an effective increase in the concentration.[42] The optical path length did not change under pressure, as the measurements were performed using a quartz cell (see Fig. S1(a), SI). The light green spectrum at 0.1 MPa, which represents the absorption after depressurization from 320 MPa, is nearly identical to that observed before pressurization, indicating that the pressure-induced changes were reversible. The fluorescence spectra exhibited two distinct emission bands in the ranges of 400–500 nm and 600–750 nm (Fig. S4, SI). The fluorescence peak also experienced bathochromic shift (Fig. S5, SI). The emission in the 600–750 nm region is attributed to the lowest singlet excited state (S_1) of the porphyrin.[43] In contrast, the emission at 400–500 nm is considered to originate from the S_2 state,[44–46] supported by the fact that the maximum emission remained constant even for different excitation wavelengths (Fig. S6, SI). The increased fluorescence intensity from the S_1 state with elevating pressure in both toluene and THF is attributed to the suppression of collisional quenching due to the increased solvent viscosity. As for the S_2 state, the fluorescence intensity decreased slightly with increasing pressure in toluene, whereas a clear enhancement was observed in THF. This could be explained by considering that the π-electron cloud in the S_2 state is influenced by pressure-induced changes in the solvent properties of toluene and THF. The excitation spectra underwent bathochromic shifts with increasing pressure (Fig. S7, SI), whereas the fluorescence lifetimes remained nearly unchanged (Fig. S8 and Table S1, SI). Hence, these results indicate that the observed spectral changes under hydrostatic pressure are typical of π-conjugated chromophores, and that pressure-induced aggregation such as π-stacking of the porphyrin units within the macrocycle did not occur. Nevertheless, the S_2 fluorescence of **2** seemed a useful fluorescence chemosensing reporter that is controllable by hydrostatic pressure.

Subsequently, both the optical and chiroptical properties of the twisted porphyrin tetramer, **1**, were investigated. The UV/vis spectra of **1** are characteristic of those of porphyrin chromophores in toluene, THF, dichloromethane (DCM), and chloroform, similar to those of the reference compound **2** (Fig. S9, left panels, SI). In all solvents, emissions from both the S_1 and S_2 excited states were observed (Fig. S9, right panels, SI) and the excitation spectra at both 0.1 and 320 MPa also exhibited slight bathochromic shifts, as also observed for **2** (Fig. S10, SI).

However, the excited-state kinetics of **1** exhibited different responses to the pressurization between halogenated and non-halogenated solvents. In toluene and THF, the fluorescence intensity of **1** increased monotonically from the S_1 state with increasing hydrostatic pressure (Fig. S9a, b; left panels, SI). In contrast, in DCM, the fluorescence decreased continuously (Fig. S9c; right panel, SI). In chloroform, the fluorescence intensity initially increased but then decreased upon pressurization (Fig. S9d; right panel, SI). The fluorescence lifetimes of **1** in toluene and THF were approximately 10 ns at atmospheric pressure, comparable to those of **2**, and remained nearly unchanged even under 320 MPa (Fig. S11a, b and Table S2, SI). On the other hand, in DCM and chloroform, the fluorescence lifetimes were shortened to 8.5 ns at atmospheric pressure and further decreased to 7.4 ns at 320 MPa (Fig. S11c, d and Table S2, SI). In DCM and chloroform, the pressure-induced conformational flexibilities in **1** may cause the solvent-mediated quenching to vary in the excited state. These findings indicate that the macrocyclic flexibility of **1** is strongly dependent on the solvent microenvironment.

Finally, the pressure-induced dynamic chiroptical behavior of **1** was investigated (Fig. 2). The clear positive Cotton effects[47] in the Soret bands of **1** at 0.1 MPa in chloroform and DCM (Fig. 2a and Fig. S12a, SI) were attributed to the (*P*)-conformer based on a previous report.[38] The CD spectra exhibited bathochromic shifts upon hydrostatic pressurization, similar to the trends observed for the UV/vis spectra. Notably, the anisotropy g ($\Delta\varepsilon/\varepsilon$) spectra around 420 nm showed a gradual increase in the g factor profiles from zero to positive values with increasing pressure (Fig. 2a). In contrast, in THF and toluene, a bisignate Cotton effect (minus-to-plus) was observed in the Soret band,[48–50] which is consistent with the (*M*)-conformer (Fig. 2b and Fig. S12b). As with the UV/vis spectra, the application of hydrostatic pressure led to a bathochromic shift in the CD spectra. Very intriguingly, the g factor profiles were found to reverse from negative to positive values and further increased upon pressurization. This inversion behavior, induced by pressure, is very rare[35] in chiroptical switchers (Fig. 3a).

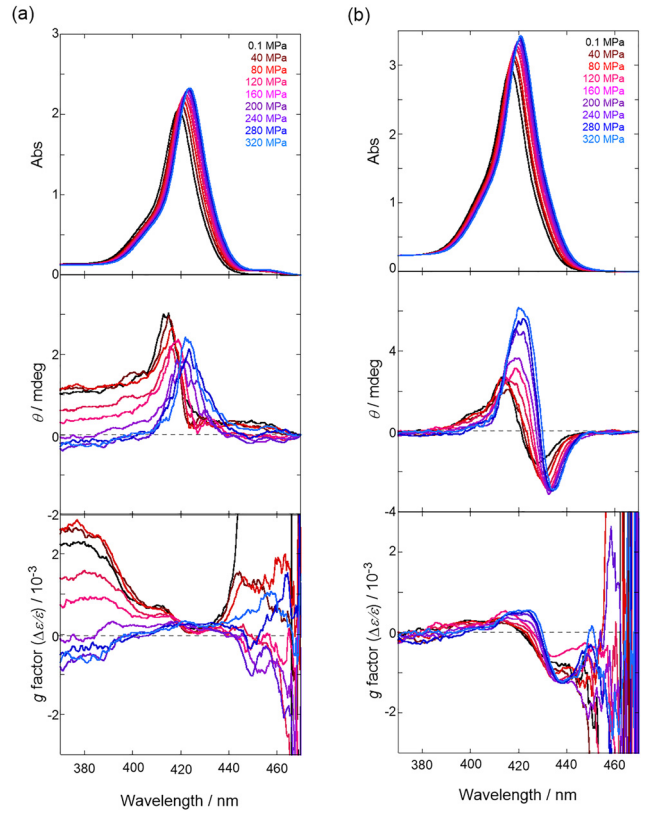

Fig. 2 Pressure-dependent UV/vis (top), CD (middle), and anisotropy *g* factor (Δε/ε) (bottom) spectra of **1** in (a) chloroform (8 μM) and (b) THF (8 μM) at room temperature at 0.1, 40, 80, 120, 160, 200, 240, 280, and 320 MPa (from black to sky blue), measured in a high-pressure cell.

The dynamic chiroptical changes exhibited by **1** can be explained by the differences in the relative stability of the (*P*)- and (*M*)-conformers arising from the solvent structure, as well as the dependence of the conformational flexibility on variations in the solvent polarity. To elucidate the origins of the dependence of the conformational flexibility of **1** on different solvents, the pressure susceptivity of the *g* factor was quantified by determining the slope of the *g* factor *versus* the pressure plot (Fig. 3b). First, a monotonic increase in the *g* factor was observed upon pressurization in all solvents, suggesting that a single mechanism is operative; that is, hydrostatic pressure promotes a more twisted molecular conformation within the same electronic state due to the inherent structural flexibility of **1**.[35,36] Second, in toluene and THF (red circles in Fig. 3b) the pressure susceptivity of **1** was higher compared to that in chloroform and DCM (blue squares in Fig. 3b). Particularly, the *g* factor underwent a sign reversal when the pressure susceptivity exceeded a threshold value of $>1.5 \times 10^{-7}$ MPa^{-1} as a chiroptical switcher. This behavior can be attributed to the pressure-induced conformational conversion of the lesser stable (*M*)-conformer into the more stable (*P*)-conformer. In both toluene and THF, the *g* factor spectra of **1** exhibited a positive increase around 420 nm and a negative decrease around 440 nm upon hydrostatic pressurization (Fig. S13, SI). Particularly in THF, an additional negative decrease was observed around 400 nm. Since the (*P*)-conformer of **1** exhibits a minus–plus–minus Cotton effect pattern,[38] the pressure-induced *g* factor changes observed in THF were interpreted as an increased population of the (*P*)-conformer, providing solid evidence of the chiroptical switching, which was reproducibly confirmed (Fig. S14, SI). The pressure-induced conformational change from the (*M*)- to the (*P*)-conformer is most likely caused by a reduction in the overall system volume due to pressure-induced desolvation,[51] since the interconversion between the two conformers involves negligible intrinsic change in molecular volume. Consequently, the sign reversal of the *g* factor of **1** in toluene and THF can be simply understood by considering that the volumetrically compact (*P*)-conformer is easier to form based on the pressure-induced release (desolvation) of solvents with lower polarities such as toluene and THF. In contrast, the conformational change induced by pressure was minimal in chloroform and DCM, as the (*P*)-conformer is already the thermodynamically favored species in these solvents, resulting in lower pressure susceptivity. These results demonstrate that **1** is capable of modulating its chiroptical responses dynamically in accordance with the solvent structure and polarity, thereby highlighting its potential as a pressure-responsive smart chiroptical material.

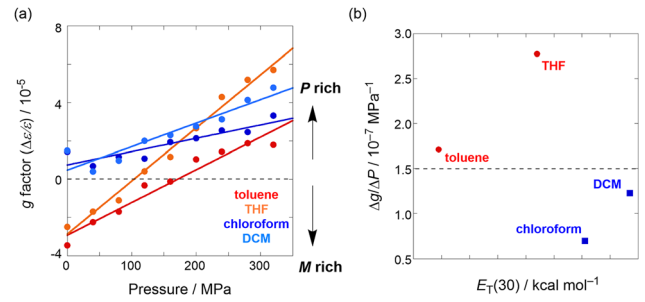

Fig. 3 (a) Pressure-dependent *g* factor (Δε/ε, peak top of 320 MPa spectra) plot of **1** in toluene, THF, chloroform, and DCM. (b) Relationship between pressure susceptivity of *g* factor and Reichardt's empirical polarity parameter (E_T(30)).[52] The dashed line indicates the threshold for chiroptical switching.

In conclusion, it was demonstrated for the first time that the chiroptical properties of **1**, with their origins in the chirally twisted structure of the porphyrin macrocycle, can be dynamically controlled by both hydrostatic pressure and the solvent microenvironment. In **1**, the twisted conformation was dependent on the solvent structures, and its CD spectra varied significantly in response to increases in the hydrostatic pressure. These findings indicate that twisted macrocycles enable the chiroptical responses to be dynamically controlled *via* hydrostatic pressurization, depending on the solvent structure and polarity. The results provide valuable insights into the rational design of pressure-induced chiroptical switching materials.

This work was supported by Grants-in-Aid (No. 23H04873, 24K21795, and 25H00897 to T. H., No. 25K18021 to N. H., and No. 23H04020, 24K01536, and 24K21791 to G. F.) from the Japan Society for the Promotion of Science (JSPS) and Tokyo

Ohka Foundation for The Promotion of Science and Technology (G. F.).

Conflicts of interest

There are no conflicts to declare.

Data availability

The data supporting this article have been included as part of supplementary information (SI). Supplementary information is available. See DOI: https://doi.org/10.1039/d5cc05443e.

Notes and references

1 I. Song, L. You, K. Chen, W. J. Lee and J. Mei, *Adv. Mater.*, 2024, **36**, e2307057.
2 G. Yang, Y. Yu, B. Yang, T. Lu, Y. Cai, H. Yin, H. Zhang, N. N. Zhang, L. Li, Y. M. Zhang and S. X. Zhang, *Angew. Chem., Int. Ed.*, 2021, **60**, 2018–2023.
3 G. Albano, G. Pescitelli and L. Di Bari, *Chem. Rev.*, 2020, **120**, 10145–10243.
4 L. A. Joyce, M. S. Maynor, J. M. Dragna, G. M. da Cruz, V. M. Lynch, J. W. Canary and E. V. Anslyn, *J. Am. Chem. Soc.*, 2011, **133**, 13746–13752.
5 N. Berova, G. Pescitelli, A. G. Petrovic and G. Proni, *Chem. Commun.*, 2009, 5958–5980.
6 Z. Dai, J. Lee and W. Zhang, *Molecules*, 2012, **17**, 1247–1277.
7 J. Lv, J. H. Han, G. Han, S. An, S. J. Kim, R. M. Kim, J. E. Ryu, R. Oh, H. Choi, I. H. Ha, Y. H. Lee, M. Kim, G. S. Park, H. W. Jang, J. Doh, J. Choi and K. T. Nam, *Nat. Commun.*, 2024, **15**, 8257.
8 Z. Feng, J. Li, P. Yang, X. Xu, D. Wang, J. Li, C. Zhang, J. Li, H. Zhang, G. Zou and X. Chen, *Nat. Commun.*, 2025, **16**, 2264.
9 H. Lee, D. Kim, J. H. Cho and J. A. Lim, *Acc. Mater. Res.*, 2025, **6**, 434–446.
10 J. W. Canary, *Chem. Soc. Rev.*, 2009, **38**, 747–756.
11 B. L. Feringa, R. A. van Delden, N. Koumura and E. M. Geertsema, *Chem. Rev.*, 2000, **100**, 1789–1816.
12 G. A. Hembury, V. V. Borovkov and Y. Inoue, *Chem. Rev.*, 2008, **108**, 1–73.
13 D. Hartmann, S. E. Penty, M. A. Zwijnenburg, R. Pal and T. A. Barendt, *Angew. Chem., Int. Ed.*, 2025, **64**, e202501122.
14 Y. Nagata, T. Nishikawa and M. Suginome, *Chem. Commun.*, 2014, **50**, 9951–9953.
15 A. H. G. David, R. Casares, J. M. Cuerva, A. G. Campaña and V. Blanco, *J. Am. Chem. Soc.*, 2019, **141**, 18064–18074.
16 K. Takaishi, M. Yasui and T. Ema, *J. Am. Chem. Soc.*, 2018, **140**, 5334–5338.
17 S. P. Morcillo, D. Miguel, L. Álvarez de Cienfuegos, J. Justicia, S. Abbate, E. Cástiglioni, C. Bour, M. Ribagorda, D. J. Cardenas, J. M. Paredes, L. Crovetto, D. Choquesillo-Lazarte, A. J. Mota, M. C. Carreño, G. Longhi and J. M. Cuerva, *Chem. Sci.*, 2016, **7**, 5663–5670.
18 H. Maeda, Y. Bando, K. Shimomura, I. Yamada, M. Naito, K. Nobusawa, H. Tsumatori and T. Kawai, *J. Am. Chem. Soc.*, 2011, **133**, 9266–9269.
19 E. Gomar-Nadal, J. Veciana, C. Rovira and D. B. Amabilino, *Adv. Mater.*, 2005, **17**, 2095–2098.
20 S. Zahn and J. W. Canary, *Science*, 2000, **288**, 1404–1407.
21 B. A. San Jose, J. Yan and K. Akagi, *Angew. Chem., Int. Ed.*, 2014, **53**, 10641–10644.
22 K. Nagai, K. Maeda, Y. Takeyama, T. Sato and E. Yashima, *Chem. – Asian J.*, 2007, **2**, 1314–1321.
23 J. Qiao, Y. He, S. Lin, Q. Fan and J. Guo, *J. Mater. Chem. C*, 2022, **10**, 7311–7318.
24 S. Du, X. Zhu, L. Zhang and M. Liu, *ACS Appl. Mater. Interfaces*, 2021, **13**, 15501–15508.
25 F. Pointillart, M. Atzori and C. Train, *Inorg. Chem. Front.*, 2024, **11**, 1313–1321.
26 Y. Wu, Z. Y. Ruan, C. Zhang, J. N. Chen, X. Y. Wang, Z. Chen, X. Gou, W. Lan, X. J. Kong, J. L. Liu, P. Cheng and W. Shi, *J. Am. Chem. Soc.*, 2025, **147**, 20799–20806.
27 P. Xue, J. Ding, P. Wang and R. Lu, *J. Mater. Chem. C*, 2016, **4**, 6688–6706.
28 A. Pucci, R. Bizzarri and G. Ruggeri, *Soft Matter*, 2011, **7**, 3689–3700.
29 Y. Sagara and T. Kato, *Nat. Chem.*, 2009, **1**, 605–610.
30 F. Meersman, C. M. Dobson and K. Heremans, *Chem. Soc. Rev.*, 2006, **35**, 908–917.
31 D. Mohammed, M. Versaevel, C. Bruyère, L. Alaimo, M. Luciano, E. Vercruysse, A. Procès and S. Gabriele, *Front. Bioeng. Biotechnol.*, 2019, **7**, 162.
32 S. E. Murthy, A. E. Dubin and A. Patapoutian, *Nat. Rev. Mol. Cell Biol.*, 2017, **18**, 771–783.
33 K. Matsumoto, K. Nakagawa, D. Asanuma and G. Fukuhara, *Front. Chem.*, 2024, **12**, 1478034.
34 J. Motoori, T. Kinoshita, H. Chai, M. S. Li, S. M. Wang, W. Jiang and G. Fukuhara, *ACS Nanosci. Au*, 2024, **4**, 435–442.
35 J. Yao, H. Mizuno, C. Xiao, W. Wu, Y. Inoue, C. Yang and G. Fukuhara, *Chem. Sci.*, 2021, **12**, 4361–4366.
36 T. Kosaka, S. Iwai, G. Fukuhara, Y. Imai and T. Mori, *Chem. – Eur. J.*, 2019, **25**, 2011–2018.
37 J. Ono, H. Sako, N. Fujisawa, M. Kitamatsu, S. Suzuki and Y. Imai, *Chem. Lett.*, 2025, **54**, upaf170.
38 K. Tanabe, N. Hisano and T. Haino, *Asian J. Org. Chem.*, 2025, **14**, e00251.
39 M. Gouterman, *J. Chem. Phys.*, 1959, **30**, 1139–1161.
40 F. A. Bovey and S. S. Yanari, *Nature*, 1960, **186**, 1042–1044.
41 T. Takagi and H. Teranishi, *J. Chem. Eng. Data*, 1982, **27**, 16–18.
42 W. W. Robertson, *J. Chem. Phys.*, 1960, **33**, 362–365.
43 J. W. Weigl, *J. Mol. Spectrosc.*, 1957, **1**, 133–138.
44 K. Hirakawa, Y. Hosokawa, Y. Nishimura and S. Okazaki, *Chem. Phys. Lett.*, 2019, **732**, 136652.
45 K. Veys and D. Escudero, *Acc. Chem. Res.*, 2022, **55**, 2698–2707.
46 R. P. Steer, *Phys. Chem. Chem. Phys.*, 2023, **25**, 23384–23394.
47 In our previous report[38] in the (*P*)-conformer, small negative Cotton effects were also observed on the shorter and longer wavelength sides of the Soret band. The different CD pattern (only visible in positive CD) is due to the large baseline noise in high-pressure CD spectroscopy. However, the positive maxima are identical to those observed as previously reported.
48 H. Gholami, D. Chakraborty, J. Zhang and B. Borhan, *Acc. Chem. Res.*, 2021, **54**, 654–667.
49 A. Dhamija, P. Mondal, B. Saha and S. P. Rath, *Dalton Trans.*, 2020, **49**, 10679–10700.
50 V. Valderrey, G. Aragay and P. Ballester, *Coord. Chem. Rev.*, 2014, **258–259**, 137–156.
51 T. Kinoshita, Y. Haketa, H. Maeda and G. Fukuhara, *Chem. Sci.*, 2021, **12**, 6691–6698.
52 C. Reichardt, *Chem. Rev.*, 1994, **94**, 2319–2358.